Journal of Power Sources 244 (2013) 17–22

Contents lists available at SciVerse ScienceDirect

Journal of Power Sources

journal homepage: www.elsevier.com/locate/jpowsour

Mn–Fe-based oxide electrocatalysts for air electrodes of lithium–air batteries

Hironobu Minowa [a,b,*], Masahiko Hayashi [a], Katsuya Hayashi [a], Ryuichi Kobayashi [a], Kazue Takahashi [a,b]

[a] NTT Energy and Environment Systems Laboratories, NTT Corporation, Morinosato-Wakamiya 3-1, Atsugi, Kanagawa 243-0198, Japan
[b] Graduate School of Natural Science and Technology, Kanazawa University, Kakuma-machi, Kanazawa, Ishikawa 920-1192, Japan

HIGHLIGHTS

- The electrochemical properties of lithium–air batteries with MnO_x were examined.
- We attempted to improve battery performance by substituting the Mn with Fe, Ni, or Co.
- The batteries using $Mn_{2-x}Fe_xO_3$ showed large 1st discharge capacity of 230 mAh g^{-1}.
- $Mn_{1.8}Fe_{0.2}O_3$ had stable cycle characteristics with a capacity loss of 25% after 10 cycles.

ARTICLE INFO

Article history:
Received 13 December 2012
Received in revised form
17 May 2013
Accepted 18 May 2013
Available online 15 June 2013

Keywords:
Lithium–air battery
Air electrode
Mn oxide
Electrocatalyst

ABSTRACT

The electrochemical properties of lithium–air batteries incorporating air electrodes loaded with MnO_x, which had different Mn valences as the electrocatalysts were examined in an organic electrolyte solution consisting of 1 mol l^{-1} lithium bis(trifluoromethanesulfonyl)imide (LiTFSI)/propylene carbonate (PC). Furthermore, we attempted to improve the battery performance by substituting the Mn site in MnO_x with Fe, Ni, or Co. The batteries using $Mn_{2-x}Fe_xO_3$ showed rather large 1st discharge capacities of 230 mAh g^{-1} at a current density of 0.25 mA cm^{-2} in a dry air atmosphere. The discharge and charge overpotentials were both greatly reduced by loading $Mn_{2-x}Fe_xO_3$ catalysts. However, almost all of these oxides exhibited poor cycle performance. Of the oxides that we examined, $Mn_{1.8}Fe_{0.2}O_3$ had comparatively stable cycle characteristics with a capacity loss of only 25% after 10 cycles.

Published by Elsevier B.V.

1. Introduction

Lithium–air batteries using ambient oxygen as a positive active material have higher energy densities than any other kind of battery, and they have been studied as promising candidates for high energy density secondary batteries [1–14]. Compared with conventional metal–air batteries, lithium–air batteries can provide a high voltage of about 3 V and a large discharge capacity by using lithium metal as a negative material. However, the batteries reported so far have shown very poor cycle performance as secondary batteries. There are many issues to be studied to overcome if we are to improve battery performance. An important battery component is the air electrode (positive electrode) on which the discharge products (LiO_x) are deposited and/or decomposed as described by the following cell reactions (discharge) [1].

$$4Li + O_2 \rightarrow 2Li_2O,\ E = 2.90\ V \quad (1)$$

$$2Li + O_2 \rightarrow Li_2O_2,\ E = 3.10\ V \quad (2)$$

The charge process whereby oxygen gas evolution occurs is expressed by the reverse reaction of the chemical formulas (1) and (2).

A highly active electrocatalyst is a very important material that enhances the reaction rate as regards both deposition and decomposition on the air electrode. Electrocatalysts are currently being investigated with special attention being paid to manganese oxides [7,8,10,14]. MnO_2 is particularly widely used because this oxide exhibits high electrocatalytic activity in relation to the

* Corresponding author. NTT Energy and Environment Systems Laboratories, NTT Corporation, Morinosato-Wakamiya 3-1, Atsugi, Kanagawa 243-0198, Japan. Tel.: +81 46 240 2699; fax: +81 46 270 2702.
E-mail address: minowa.hironobu@lab.ntt.co.jp (H. Minowa).

0378-7753/$ – see front matter Published by Elsevier B.V.
http://dx.doi.org/10.1016/j.jpowsour.2013.05.075

decomposition of the discharge product. Debart et al. [7] reported that a lithium–air battery with electrolytic manganese dioxide as an electrocatalyst achieved 100 cycles (600 mAh g^{-1}-carbon) in a discharge–charge test. Mizuno et al. [14] also did the same supplementary examination as Debart et al. Thapa et al. [8] also reported that MnO_2 modified by Pd had a stable capacity of 225 mAh g^{-1} (total weight of air electrode) during 20 cycles owing to its small charge potential of 3.7 V. Read et al. [10] reported that λ-MnO_2 had first discharge capacity of >1000 mAh g^{-1}-carbon. In this study, first, we investigated the battery performance of a lithium–air battery using MnO_x, which has different manganese valences when calcined in various atmospheres. Then, we attempted to improve the battery performance by substituting the Mn site in MnO_x with Fe, Ni, or Co. Finally, the substitution rate was evaluated to determine a suitable composition for the electrocatalysts of air electrodes.

2. Experimental

The Mn–Fe-based oxides, $Mn_{2-x}Fe_xO_3$, were prepared by using an amorphous malate precursor method as reported elsewhere [15–18]. The amorphous precursor powder was obtained by evaporating a mixed aqueous solution of metal nitrates of Mn, Fe, Ni, Co and malic acid. The amorphous powder was calcined at 500, 650, 800, or 950 °C for 5 h in H_2, air and O_2. The crystalline structures of the calcined powders were confirmed by using an X-ray diffractometer (Rigaku Co., RINT2500, X-ray radiation: CuK_α). The specific surface areas (SSAs) of the oxides were measured by using a Brunauer–Emmett–Teller (BET) analysis system (Tristar 3000, Shimadzu Co.) with an N_2 adsorptive medium.

The air electrodes were prepared by the following procedure. A mixture of the oxide powder, carbon powder and PTFE powder (weight ratio of 5:3:2) was rolled into a 0.5 mm thick sheet and cut into 16 mm diameter pellets, which were then pressed on a Ti mesh. The high-surface-area carbon black, Ketjen Black EC600JD (1270 m^2 g^{-1}, Lion Co.), was used as the carbon powder for the air electrode.

The lithium–air cell was composed of an air electrode, a lithium metal sheet (0.6 mm thick) and 1 mol l^{-1} LiTFSI/PC as a positive electrode, a negative electrode and an electrolyte solution, respectively, as shown in Fig. 1. A propylene membrane (Celgard3501, Celgard, LLC.) was used as a separator. The cell was constructed by stacking the air electrode, the separator immersed in the electrolyte solution and the lithium sheet in series. One side of the air electrode was exposed to an ambient atmosphere. The electrochemical tests were carried out in dry air with a dew point of less than −50 °C.

Discharge–charge measurements were carried out under a galvanostatic condition in a 2.0–4.5 V range at room temperature. The current density was 0.25 mA cm^{-2}. The discharge and charge capacities were normalized by the total weight of the air electrode.

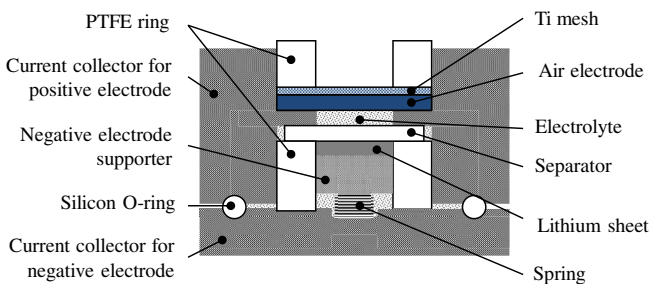

Fig. 1. Schematic diagram of a lithium–air battery.

In addition, the electrolyte was extracted from the lithium–air cell after the discharge–charge cycle test and the amount of Mn dissolution was estimated by analyzing the electrolyte solution with the Inductively Coupled Plasma Mass Spectrometry (ICP-MS) method (Agilent 7500cs, Agilent Technologies, Inc.).

3. Results and discussion

3.1. Electrochemical performance of MnO_x electrocatalysts

Fig. 2 shows XRD patterns of manganese oxide (MnO_x) powder calcined at 500 °C for 5 h in various atmospheres. MnO_x was identified as MnO (PDF no. 75-6876), Mn_2O_3 (no. 73-1826) and MnO_2 (no. 71-0071) at the calcination temperatures of H_2, air and O_2, respectively. No peaks corresponding to impurity phases were observed in the XRD patterns of the other oxides. The crystallite diameter of MnO, Mn_2O_3 and MnO_2 calculated by Scherrer's formula from the XRD patterns were 508, 310 and 212 Å, respectively. Manganese oxides, which had three types of valence (Mn^{2+}, Mn^{3+}, Mn^{4+}), could be prepared by calcining in various atmospheres.

Fig. 3(a) shows the typical first discharge and charge curves of lithium–air batteries incorporating air electrodes loaded with MnO_x. Mn_2O_3 exhibited the largest discharge capacity of over 160 mAh g^{-1} and a smaller difference between the charge and discharge overpotentials (discharge plateau voltage: 2.65 V, charge plateau voltage: 4.10 V). Although capacities are lower than previous reported capacities [12], this is because the use of the air electrode with the oxide which has large particle size decrease in the number of reaction sites. On the other hand, MnO_2 exhibited plateau voltages of about 2.55 V for is charging and about 4.20 V for charging. MnO had the smallest discharge capacity and no discharge or charge plateau voltages for either discharging or charging.

Fig. 3(b) shows the cycle characteristics of lithium–air batteries incorporating air electrodes loaded with MnO_x. Mn_2O_3 showed the largest capacity after the 10th cycle of the MnO_x that we tested. Although there have been some reports stating that lithium–air batteries incorporating air electrodes loaded with MnO_2 provide good cycle performance [6–8,10,11,14], Mn_2O_3 exhibited the smallest difference in terms of overpotential, a larger discharge capacity and better cycle performance than MnO_2 in this study. As a result, it seems that an oxide with a small particle size dispersed in

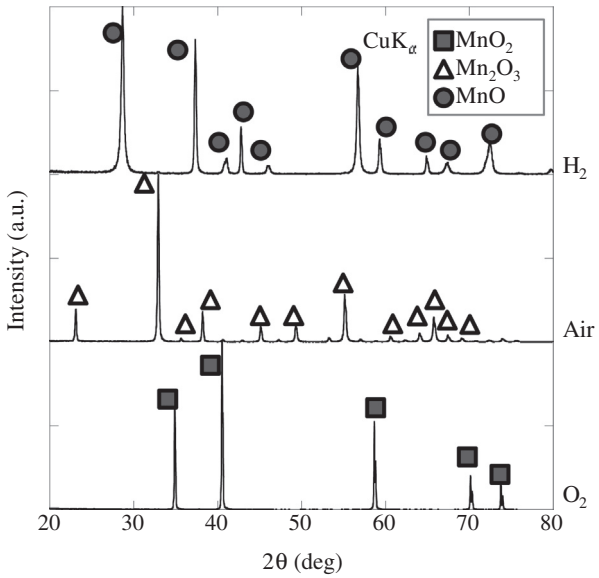

Fig. 2. XRD patterns of MnO_x calcined in various atmospheres.

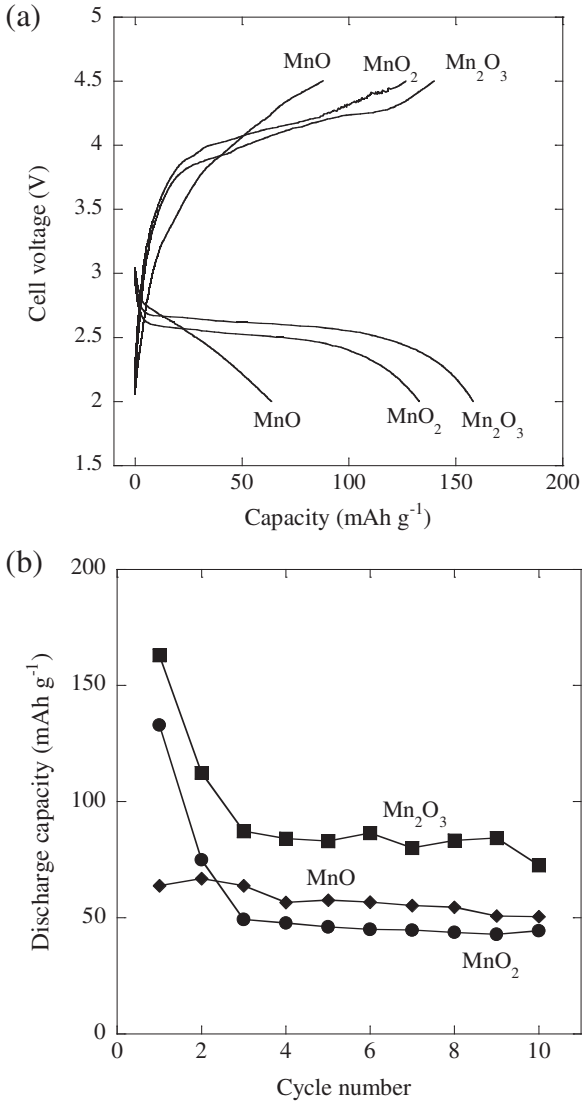

Fig. 3. (a) The first discharge–charge curves and (b) cycle performance of lithium–air batteries incorporating air electrodes loaded with MnO, Mn_2O_3, and MnO_2.

air electrode and extensively worked as an electrocatalyst. Also, it is likely that the MnO_x of Mn^{3+} exhibited better cycle performance than Mn^{4+} as an electrocatalyst. This is because we have already reported that perovskite-type oxides, $La_{0.6}Sr_{0.4}Fe_{0.6}Mn_{0.4}O_3$ (Mn valence: 3.4+), exhibited good cycle performance as electrocatalysts [13]. Therefore, we investigated Mn_2O_3 in more detail.

3.2. Electrochemical performance of lithium–air batteries using manganese-based oxide electrocatalysts

We attempted to improve battery performance by substituting the Mn site in Mn_2O_3 with Fe, Ni, or Co. Fig. 4 shows XRD patterns of Mn-based oxide ($Mn_{1.8}M_{0.2}O_3$ (M = Fe, Mn, Ni, Co)) powder calcined at 500 °C for 5 h in air. $Mn_{1.8}Fe_{0.2}O_3$, $Mn_{1.8}Ni_{0.2}O_3$, and $Mn_{1.8}Co_{0.2}O_3$ had crystallite diameters of 264, 292 and 277 Å, respectively. There is no new crystal phase with Fe substitution. In contrast, Co or Ni substitution produces a new phase such as $MnCo_2O_4$ or Ni_6MnO_8. Furthermore the mixed phase indicates that no solid pure solution of Mn_2O_3 was formed in these oxides substituted with Co or Ni. Although Mn_2O_3 substituted with Ni and

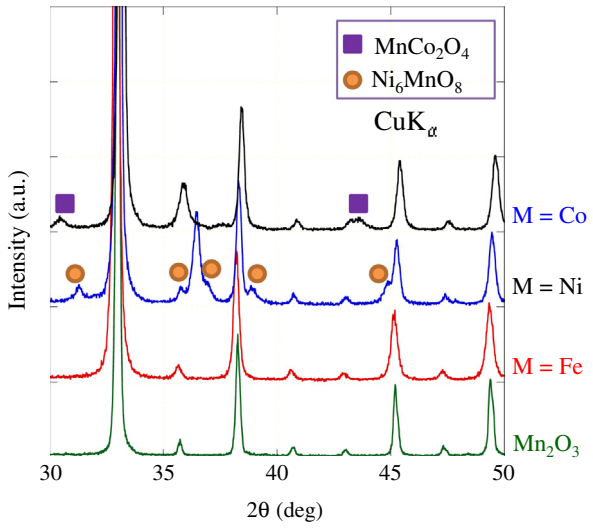

Fig. 4. XRD patterns of $Mn_{1.8}M_{0.2}O_3$ (M = Fe, Mn, Ni, Co) powders.

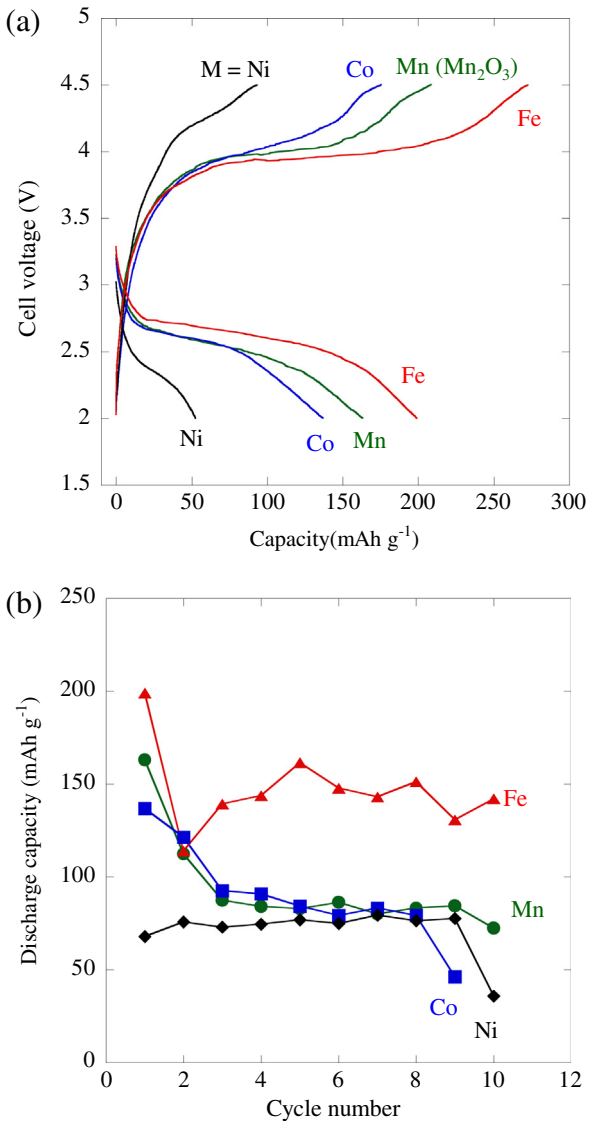

Fig. 5. (a) The first discharge–charge curves and (b) cycle performance of lithium–air batteries incorporating air electrodes loaded with $Mn_{1.8}M_{0.2}O_3$ (M = Fe, Mn, Ni, Co).

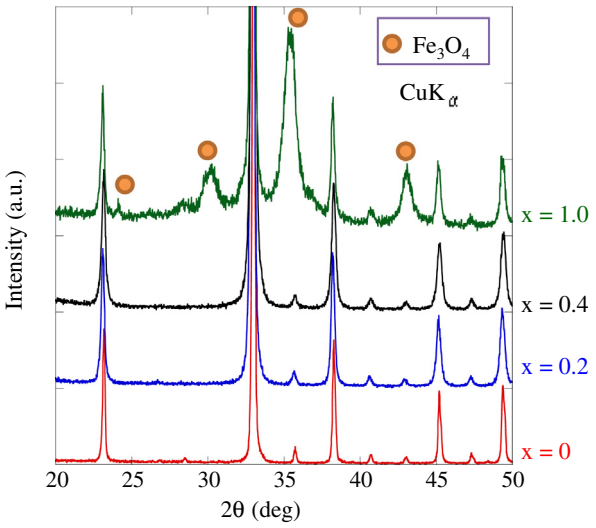

Fig. 6. XRD patterns of $Mn_{2-x}Fe_xO_3$ (x = 0, 0.2, 0.4, 1.0) powders.

Co has a mixed phase, these are simply represented as $Mn_{1.8}Ni_{0.2}O_3$ and $Mn_{1.8}Co_{0.2}O_3$, respectively.

Fig. 5(a) shows the first discharge and charge curves of lithium–air batteries incorporating air electrodes loaded with $Mn_{1.8}M_{0.2}O_3$ (M = Fe, Mn, Ni, Co). $Mn_{1.8}Fe_{0.2}O_3$ provides the largest capacity of over 200 mAh g^{-1} and the smallest difference between the charge and discharge overpotentials. On the other hand, $Mn_{1.8}Co_{0.2}O_3$ and $Mn_{1.8}Ni_{0.2}O_3$ exhibited a smaller capacity and a larger overpotential than unsubstituted Mn_2O_3. Fig. 5(b) shows the cycle characteristics of lithium–air batteries incorporating air electrodes loaded with $Mn_{1.8}M_{0.2}O_3$ (M = Fe, Mn, Ni, Co). $Mn_{1.8}Fe_{0.2}O_3$ had the largest capacity after the 10th cycle. This suggests that $Mn_{1.8}Fe_{0.2}O_3$ exhibits higher electrocatalytic activity as regards oxygen reduction (discharge) and evolution (charge) than Mn_2O_3. On the other hand, $Mn_{1.8}Co_{0.2}O_3$ and $Mn_{1.8}Ni_{0.2}O_3$ exhibited a smaller capacity and a larger overpotential than Mn_2O_3. It appears that the impurities in $Mn_{1.8}Co_{0.2}O_3$ and $Mn_{1.8}Ni_{0.2}O_3$ induce less electrocatalytic activity in terms of electrode reactions than Mn_2O_3.

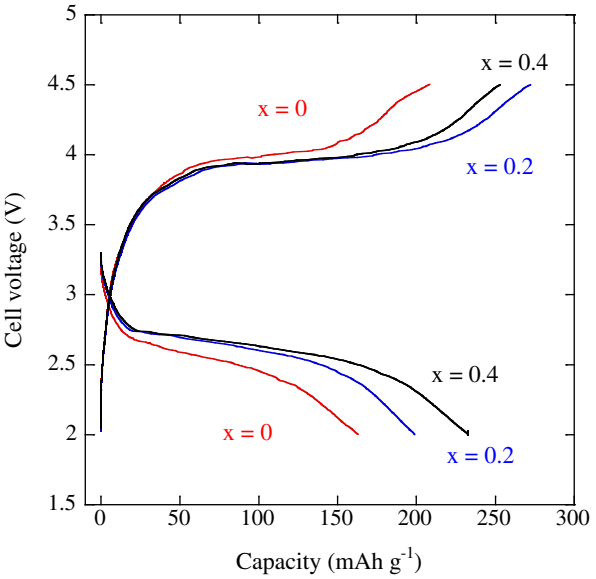

Fig. 7. The first discharge–charge curves of lithium–air batteries incorporating air electrodes loaded with $Mn_{2-x}Fe_xO_3$ (x = 0, 0.2, 0.4).

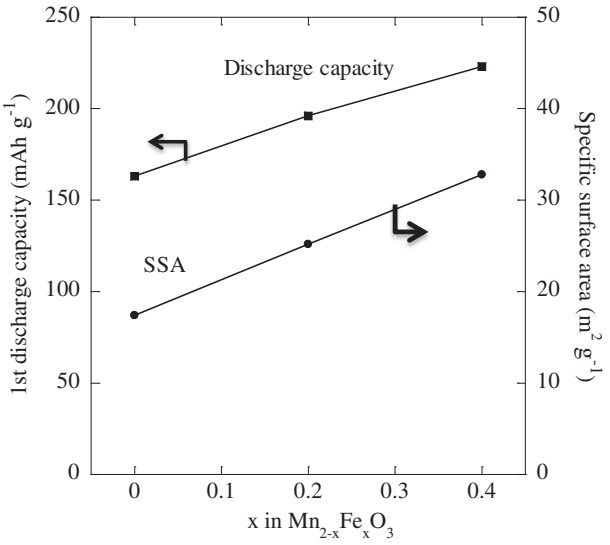

Fig. 8. The 1st discharge capacities of lithium–air batteries with $Mn_{2-x}Fe_xO_3$ (x = 0, 0.2, 0.4) and the SSA of these oxide powders.

3.3. Improvement by optimizing Fe substitution content in Mn_2O_3

We attempted to achieve further improvement by optimizing the Fe substitution content in Mn_2O_3. Fig. 6 shows XRD patterns and the SSA of $Mn_{2-x}Fe_xO_3$ ($0 \leqq x \leqq 1.0$) calcined at 500 °C in air. $Mn_{1.6}Fe_{0.4}O_3$ and $Mn_{1.0}Fe_{1.0}O_3$ had crystallite diameters of 243 and 199 Å, respectively. As a result, the oxides at x = 0, 0.2 and 0.4 could be formed as solid solutions of Mn_2O_3 without an impurity phase. However, this confirmed that the crystal phase of the sample at x = 1.0 was a mixed phase because oxides could not be formed as a solid solution of Mn_2O_3. Therefore, we examined samples with x = 0 (Mn_2O_3), 0.2 ($Mn_{1.8}Fe_{0.2}O_3$) and 0.4 ($Mn_{1.6}Fe_{0.4}O_3$) but not with x = 1.0.

Fig. 7 shows the 1st charge–discharge curves of lithium–air batteries with $Mn_{2-x}Fe_xO_3$ electrocatalysts x = 0, 0.2 and 0.4. The overpotential became small when we used Mn_2O_3 substituted by Fe as an electrocatalyst. In particular, $Mn_{1.8}Fe_{0.2}O_3$ and $Mn_{1.6}Fe_{0.4}O_3$

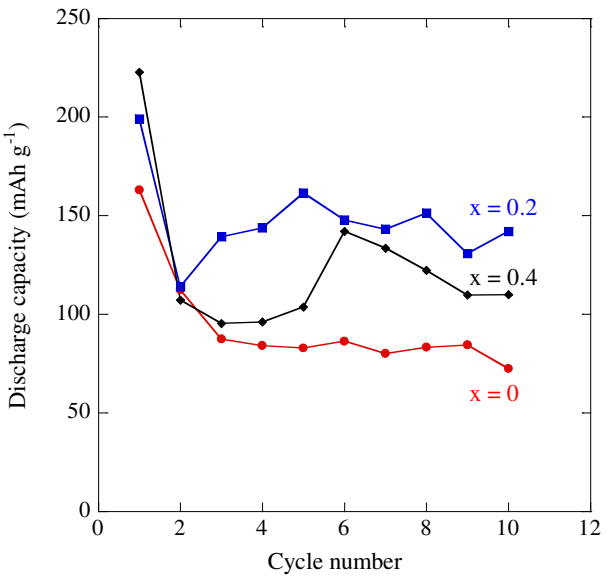

Fig. 9. Cycle performance of lithium–air batteries incorporating air electrodes loaded with $Mn_{2-x}Fe_xO_3$ (x = 0, 0.2, 0.4).

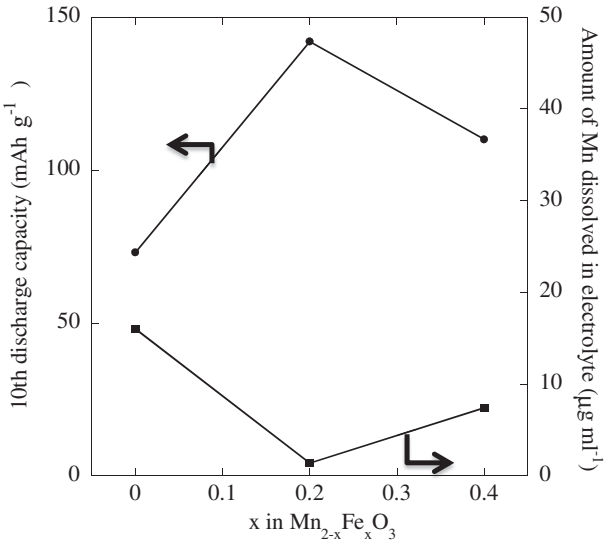

Fig. 10. The 10th discharge capacities of lithium–air batteries with $Mn_{2-x}Fe_xO_3$ ($x = 0$, 0.2, 0.4) and the amount of Mn dissolved from these oxide powders into the electrolyte after 10th discharge–charge cycle.

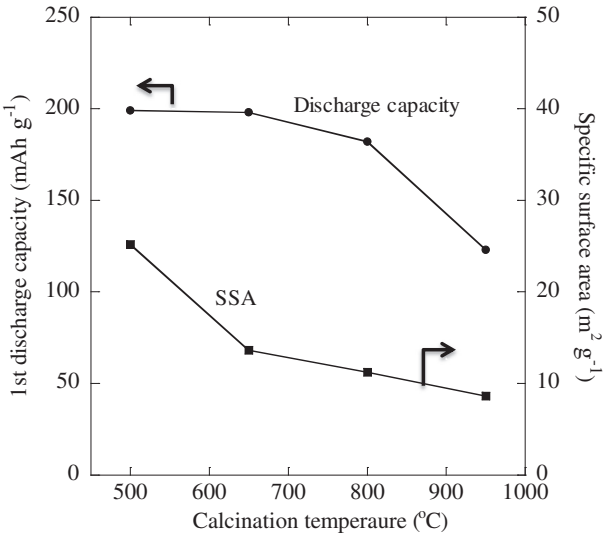

Fig. 12. The 1st discharge capacities of lithium–air batteries with $Mn_{1.8}Fe_{0.2}O_3$ calcined at 500, 650, 800 and 950 °C and the SSA of these oxides powders.

exhibited a smaller difference in their overpotentials for charging and discharging. The batteries had a larger 1st discharge capacity with the oxide electrocatalysts when x was increased. The batteries using $Mn_{1.6}Fe_{0.4}O_3$ had the largest capacity of 230 mAh g^{-1}.

Fig. 8 shows the correlation between the 1st discharge capacity and the SSAs of the oxides. The oxide with the higher SSA had a larger 1st discharge capacity when using the oxide electrocatalysts calcined at a lower temperature. It appeared that the highly active oxide particles were homogeneously dispersed by using an electrocatalyst with a high SSA and the reaction sites were widely formed. Fig. 9 shows the cycle properties of lithium–air batteries using $Mn_{2-x}Fe_xO_3$. The battery using $Mn_{1.8}Fe_{0.2}O_3$ exhibited the best cycle performance although the battery using $Mn_{1.6}Fe_{0.4}O_3$ exhibited the largest capacity at the 1st discharge. Although the cycle performance was improved by using $Mn_{2-x}Fe_xO_3$ electrocatalyst, the batteries exhibited different characteristics. Then, we investigated the stability of $Mn_{2-x}Fe_xO_3$ by measuring the amount of Mn that dissolved in the electrolyte.

Fig. 10 shows the correlation between the 10th discharge capacity and the amount of Mn dissolved in the electrolyte. The battery using $Mn_{1.8}Fe_{0.2}O_3$ electrocatalyst provided the best cycle performance. This oxide had the smallest amount of Mn dissolved in the electrolyte and the largest capacity after 10 cycles. The cycle performance tended to improve when less Mn was dissolved in the electrolyte. It appears that the electrochemical stability of the oxide electrocatalyst affects battery performance.

3.4. Effects of $Mn_{1.8}Fe_{0.2}O_3$ calcination temperatures

Fig. 11 shows the 1st discharge–charge curves of lithium–air batteries with $Mn_{1.8}Fe_{0.2}O_3$ electrocatalysts calcined at various temperatures. The charge and discharge overpotentials decreased

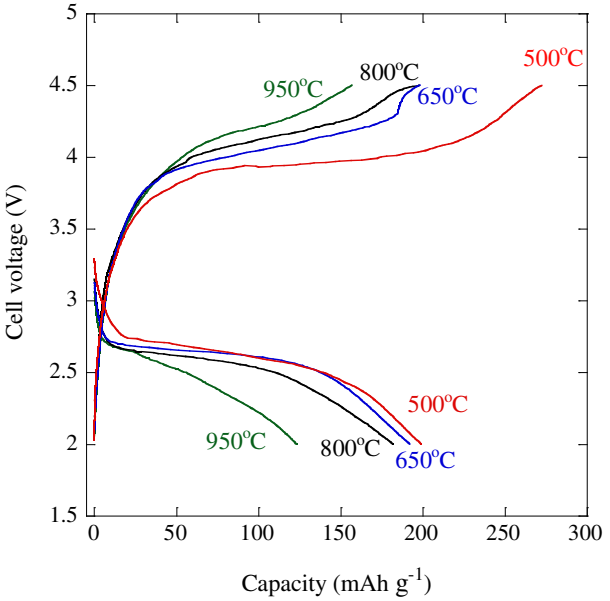

Fig. 11. The first discharge–charge curves of lithium–air batteries incorporating air electrodes loaded with $Mn_{1.8}Fe_{0.2}O_3$ calcined at 500, 650, 800 and 950 °C.

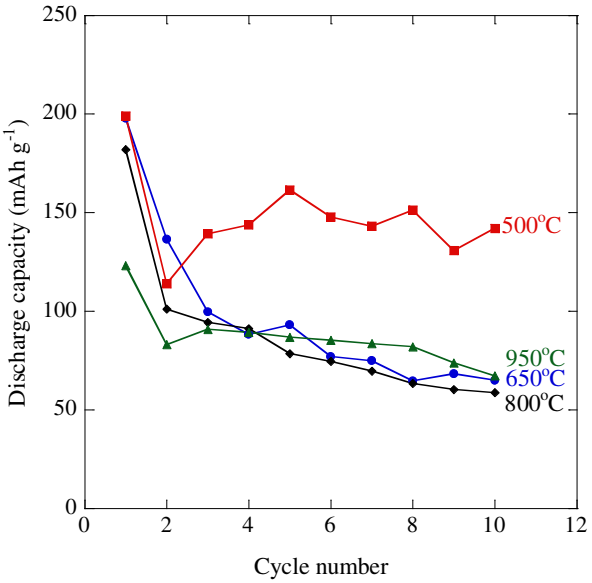

Fig. 13. Cycle performance of lithium–air batteries incorporating air electrodes loaded with $Mn_{1.8}Fe_{0.2}O_3$ calcined at 500, 650, 800 and 950 °C.

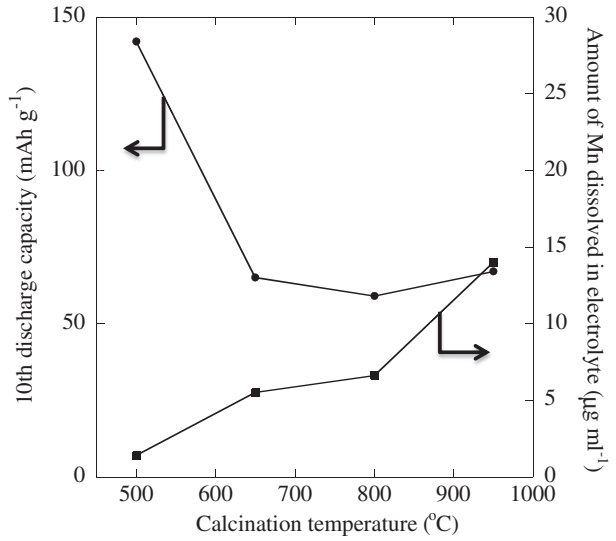

Fig. 14. The 10th discharge capacities of lithium–air batteries with $Mn_{1.8}Fe_{0.2}O_3$ calcined at 500, 650, 800 and 950 °C and the amount of Mn dissolved from these oxide powders into the electrolyte after 10th discharge–charge cycle.

by using $Mn_{1.8}Fe_{0.2}O_3$ calcined at lower temperature. In particular, the charge overpotential decreased when $Mn_{1.8}Fe_{0.2}O_3$ calcined at 500 °C was used as an electrocatalyst. Moreover, $Mn_{1.8}Fe_{0.2}O_3$ electrocatalyst calcined at lower temperature exhibited large discharge and charge capacities. Lithium–air batteries using $Mn_{1.8}Fe_{0.2}O_3$ calcined at 500 °C exhibited a discharge capacity of about 200 mAh g^{-1}.

Fig. 12 shows the correlation between the 1st discharge capacities and the SSAs of the oxides. A larger 1st discharge capacity was obtained when the SSA was lower. The use of an electrocatalyst with a high SSA appears to increase the number of reaction sites and their dispersion because this result exhibited the same tendency as seen in Fig. 10.

Fig. 13 shows the cycle properties of lithium–air batteries with $Mn_{1.8}Fe_{0.2}O_3$ electrocatalysts calcined at 500, 650, 800 and 950 °C. The battery using $Mn_{1.8}Fe_{0.2}O_3$ electrocatalyst calcined at 500 °C had the most stable cycle performance after the 10th cycle. We investigated the stability of $Mn_{1.8}Fe_{0.2}O_3$ by measuring the amount of Mn that dissolved in the electrolyte. Fig. 14 shows the correlation between the 10th discharge capacity and the amount of Mn dissolved in the electrolyte, which increased with increasing calcination temperature. As a result, $Mn_{1.8}Fe_{0.2}O_3$ calcined at 500 °C exhibited the smallest amount of Mn dissolution. It appears that the electrochemical stability of the oxide electrocatalyst affected the cycle characteristics.

4. Conclusions

Mn–Fe-based oxides were found to exhibit good activity as electrocatalysts for the air electrodes of lithium–air batteries. Of these oxides, $Mn_{1.8}Fe_{0.2}O_3$ showed the most stable cycle characteristics. A lithium–air battery incorporating an air electrode loaded with this oxide had a discharge capacity of about 150 mAh g^{-1} at the 10th discharge. Moreover, the cycle performance tended to improve when less Mn was dissolved in the electrolyte. These results suggest that the electrochemical stability of the Mn-based oxide electrocatalyst influenced the cycle characteristics.

Acknowledgments

We are grateful to Dr. Yasuyuki Sugiyama of NTT Energy and Environment Systems Laboratories for helpful guidance and discussions. We also thank Mr. Hirokuni Ota and Taiki Yamada for their assistance with the experiments.

Appendix A. Supplementary data

Supplementary data related to this article can be found at http://dx.doi.org/10.1016/j.ejmech.2013.06.011.

References

[1] K.M. Abraham, Z. Jiang, J. Electrochem. Soc. 143 (1996) 1.
[2] T. Kuboki, T. Okuyama, T. Ohsaki, N. Takami, J. Power Sources 146 (2005) 766.
[3] Y. Wang, H. Zhou, J. Power Sources 195 (2009) 358.
[4] A. Dobley, C. Morein, R. Roark, in: 210th Meeting of Electrochemical Society, Abstract #391, 2006.
[5] Y. Lu, H.A. Gasteiger, Y. Shao-Horna, Electrochem. Solid-state Lett. 14 (2011) A70.
[6] T. Ogasawara, A. Debart, M. Holzapfel, P. Novak, P.G. Bruce, J. Am. Chem. Soc. 128 (2006) 1390.
[7] A. Debart, J. Bao, G. Armstrong, P.G. Bruce, J. Power Sources 174 (2007) 1177.
[8] A.K. Thapa, K. Saimen, T. Ishihara, Electrochem. Solid-state Lett. 13 (2010) A165.
[9] T. Zhang, N. Imanishi, S. Hasegawa, A. Hirano, J. Xie, Y. Takeda, O. Yamamoto, N. Sammes, J. Electrochem. Soc. 155 (2008) A965.
[10] J. Read, J. Electrochem. Soc. 149 (2002) A1190.
[11] S.S. Zhang, D. Foster, J. Read, J. Power Sources 195 (2010) 1235.
[12] M. Hayashi, H. Minowa, M. Takahashi, T. Shodai, Electrochemistry 78 (2010) 325.
[13] H. Minowa, M. Hayashi, M. Takahashi, T. Shodai, Electrochemistry 78 (2010) 353.
[14] F. Mizuno, S. Nakanishi, Y. Kotani, S. Yokoishi, H. Iba, Electrochemistry 78 (2010) 403.
[15] Y. Shimizu, H. Matsuda, A. Nemoto, N. Miura, N. Yamazoe, Prog. Batteries Battery Mater. 12 (1993) 108.
[16] Y. Matsumoto, H. Yoneyama, H. Tamura, J. Electroanal. Chem. 83 (1977) 245.
[17] N. Miura, M. Hayashi, T. Hyodo, N. Yamazoe, Mater. Sci. Forum 315–317 (1999) 562.
[18] Y. Teraoka, H. Kanebayashi, I. Moriguchi, S. Kagawa, Chem. Lett. 1991 (1991) 673.